

Relationship Between Static, Flight, and Simulated Flight Jet Noise Measurements

R. S. McGowan* and R. S. Larson†

Pratt & Whitney Aircraft Group, East Hartford, Connecticut

Jet noise data are acquired in three different forms: static, flight, and simulated forward flight. Often data must be transformed from one type to one of the other two. A number of studies exist defining the relationship between these three types of measurements. These studies are deficient because they do not explicitly consider the jet noise source characteristics or do not clearly distinguish between mean square pressure, power spectral density, and one-third octave band sound pressure level measurements. In the current study, the relationships between static, subsonic flight, and subsonic simulated forward flight one-third octave band sound pressure level measurements were defined.

I. Introduction

JET noise data are acquired in three different forms: static data (Fig. 1) obtained from a model nozzle or full-scale engine operated in a quiescent atmosphere; flight data (Fig. 2) acquired from a full-scale engine in flight; and simulated forward flight data (Fig. 3) obtained from a model nozzle placed in a larger nozzle flow that simulates the effect of flight. Often data acquired in one manner must be transformed to one of the other two situations. For example, static or simulated forward flight data are often transformed to flyover data, after an appropriate extrapolation. Therefore, differences between these situations must be defined.

The current literature contains numerous studies of the prediction of flyover noise measurements from static measurements, including studies by Cocking,¹ Morfey,² and Crighton.³ However, these studies lack clarity because they use calculations based on nonaerodynamic noise sources (Ref. 3, for example) or they do not clearly distinguish between mean square pressure, power spectral density, or one-third octave band sound pressure level measurements (Refs. 1, 2, and 4, for example). The current study was undertaken to clarify the relationship of the three types of one-third octave band sound pressure level measurements using Lighthill's⁵ formulation of the jet noise generation process. In the next section, Lighthill's analysis of the static case is outlined, Ffowcs William's⁶ and Ribner's⁷ analysis of the subsonic flight case is outlined, and the analysis of the subsonic simulated flight case is presented. The three analyses are compared in Sec. III and the Michalke and Michel⁴ results are compared to the current study. Conclusions are contained in Sec. IV.

II. Analysis

Static Jet Noise

In the classic paper by Lighthill,⁵ the noise radiated from the turbulence generated in the exhaust plume of an engine is given by

$$(\rho - \rho_0)\{x, t\} = \frac{1}{4\pi c_0^2} \int \frac{\partial^2}{\partial x_i \partial x_j} T_{ij}(y, \tau_y) \frac{d^3 y}{|x - y|} \quad (1)$$

where $\rho - \rho_0$ is the density fluctuation, ρ_0 and c_0 the ambient

air density and speed of sound, respectively, x the observation point, and y the source integration variable. The quantity T_{ij} is the stress tensor approximated by $T_{ij} = \rho_0 u_i u_j$, where u_i , $i = 1, 2, 3$ are the turbulence velocity components; the quantity τ_y is given by

$$\tau_y = t - (1/c_0) |x - y| \quad (2)$$

The spatial derivatives in Eq. (1) can be converted to time derivatives using Eq. (2) yielding the equation

$$(\rho - \rho_0)\{x, t\} = \frac{1}{4\pi c_0^2} \int \frac{\partial \tau_y}{\partial x_i} \frac{\partial \tau_y}{\partial x_j} \frac{\partial^2}{\partial \tau_y^2} T_{ij}(y, \tau_y) \frac{d^3 y}{|x - y|} \quad (3)$$

The solution desired is an expression for the mean square pressure, which can be obtained by squaring Eq. (3) and time averaging the result. The dynamics of the solution associated with the convection velocity of the source can be defined by transforming the resulting integrals to a coordinate frame fixed with respect to the convecting turbulence. The procedure for doing this will be outlined for comparison with similar steps in the next two sections.

The acoustic autocorrelation is defined by, if the turbulence is stationary,

$$\begin{aligned} \langle p_s^2(x, \tau^*) \rangle &= c_0^2 \langle (\rho - \rho_0)\{x, t\} (\rho - \rho_0)\{x, t + \tau^*\} \rangle \\ &= \frac{1}{16\pi^2 c_0^6} \int \frac{d^3 y}{|x - y|} \int \frac{d^3 z}{|x - z|} \frac{\partial \tau_y}{\partial x_i} \frac{\partial \tau_y}{\partial x_j} \frac{\partial \tau_z}{\partial x_k} \frac{\partial \tau_z}{\partial x_l} \\ &\quad \times \left\langle \frac{\partial^2}{\partial \tau_y^2} T_{ij}^s(y, \tau_y) \frac{\partial^2}{\partial \tau_z^2} T_{kl}^s(z, \tau_z) \right\rangle \end{aligned} \quad (4)$$

where $\tau_z = t + \tau^* - |x - z|/c_0$, the autocorrelation time delay is τ^* , and the subscript s was used to indicate the static solution. Assuming that the turbulence is stationary, one may write

$$\left\langle \frac{\partial^2 T_{ij}^s(y, \tau_y)}{\partial \tau_y^2} \frac{\partial^2 T_{kl}^s(z, \tau_z)}{\partial \tau_z^2} \right\rangle = \frac{\partial^4}{\partial \tau^{*4}} R_{ijkl}(y, \Delta, \tau)$$

where

$$\begin{aligned} R_{ijkl} &= \langle T_{ij}(y, \tau_y) T_{kl}(z, \tau_z) \rangle \\ \tau &= \tau_z - \tau_y = \tau^* + \frac{|x - y| - |x - z|}{c_0} \end{aligned} \quad (5)$$

and

$$\Delta = z - y$$

Received June 29, 1981; revision received July 7, 1983. Copyright © American Institute of Aeronautics and Astronautics, Inc., 1983. All rights reserved.

*Senior Engineer; currently Instructor of Mathematics, Connecticut College, New London, Conn.

†Research Engineer; currently Director, Management Science, Heublein, Inc., Hartford, Conn.

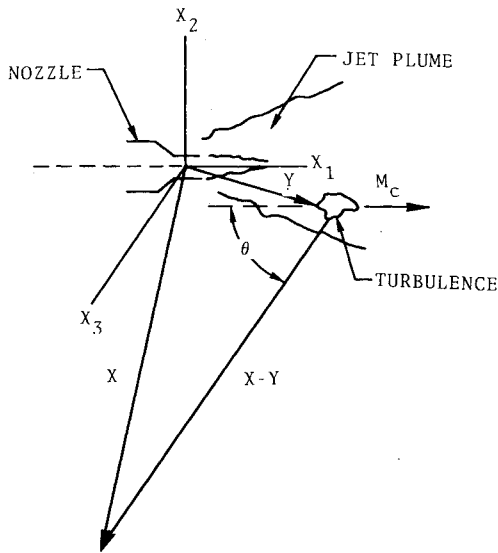


Fig. 1 Geometry in a static jet noise test.

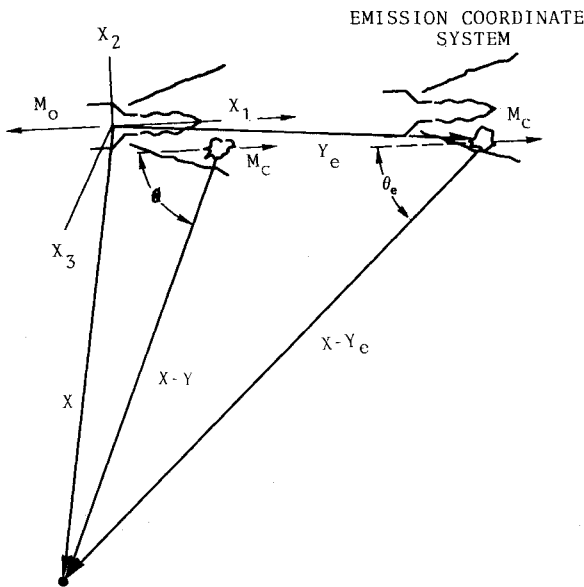


Fig. 2 Geometry in a flight jet noise test.

In the far field, Eq. (4) becomes

$$\langle p_s^2(x, \tau^*) \rangle = \frac{1}{16\pi^2 c_0^6} \int \frac{d^3 y}{|x-y|^2} \int d^3 \Delta \frac{\partial \tau_y}{\partial x_i} \frac{\partial \tau_y}{\partial x_j} \frac{\partial \tau_z}{\partial x_k} \frac{\partial \tau_z}{\partial x_l} \times \frac{\partial^4}{\partial \tau^4} R_{ijkl}(y, \Delta, \tau) \quad (6)$$

As stated earlier, to fully illustrate the effects of the turbulence convection on the acoustic autocorrelation, the integration in Eq. (6) is now transformed to an integration in a frame of reference moving at the turbulence convection velocity. Let

$$\Delta = \lambda + V_c \tau = \lambda + M_c c_0 \tau \quad (7)$$

where V_c is the turbulence convection velocity and M_c is the convection Mach number, referenced to the ambient speed of sound and measured with respect to a nozzle-fixed coordinate frame. Equation (4) can now be transformed to define the

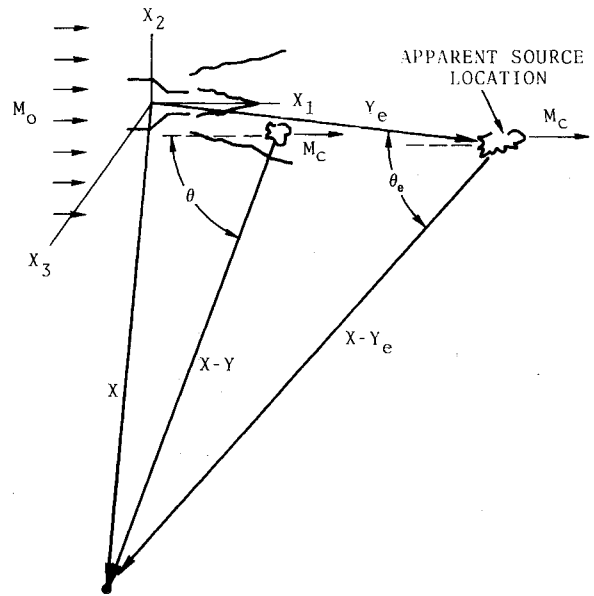


Fig. 3 Geometry in a simulated forward flight jet noise test.

dynamic effects of the turbulence convection velocity on the far-field noise directivity. Assuming that the turbulence correlation lengths are small with respect to the distance from the source to the observer,

$$d^3 \Delta = d^3 \lambda / (1 - M_c \cos \theta), \quad \frac{\partial \tau_z}{\partial x_i} \approx \frac{\partial \tau_y}{\partial x_i} = -\frac{1}{c_0} \frac{x_i - y_i}{|x - y|} \quad (8)$$

and

$$\frac{\partial}{\partial \tau} R_{ijkl}(y, \Delta, \tau) = \frac{1}{1 - M_c \cos \theta} \frac{\partial}{\partial \tau} P_{ijkl}(y, \lambda, \tau)$$

where P_{ijkl} is the representation of R_{ijkl} in the λ coordinate frame. Thus, Eq. (4) becomes

$$\langle p_s^2(x, \tau^*) \rangle = \frac{1}{16\pi^2 c_0^6} \int \frac{d^3 y}{|x-y|^2} \frac{Q^s(x, y, \tau)}{(1 - M_c \cos \theta)^5} \quad (9)$$

where

$$Q^s(x, y, \tau) = \frac{(x_i - y_i)(x_j - y_j)(x_k - y_k)(x_l - y_l)}{|x - y|^4} \times \int d^3 \lambda \frac{\partial^4}{\partial \tau^4} P_{ijkl}(y, \lambda, \tau)$$

and the notation s indicates the static solution. The relationship between τ and τ^* can be determined from Eqs. (5) and (7). That is, in the far field and for a localized region of turbulence, $\tau = \tau^* / (1 - M_c \cos \theta) + O(\lambda/c_0)$.

Equation (9) can be used to define the static power spectral density, $\langle p_s^2(x, \omega) \rangle$, from which, in turn, the one-third octave band sound pressure level, SPL(x, ω) can be obtained. The one-third octave band sound pressure level is the quantity usually measured in static and flight tests and the results derived here will be used in Sec. III to derive in detail the relationship between static, flight, and simulated forward flight one-third octave band sound pressure level measurements. The first step is to derive an expression for the power spectral density, which is obtained by taking the Fourier transform in Eq. (9). The result is

$$\begin{aligned}
\langle p_s^2(x, \omega) \rangle &= \frac{I}{16\pi^2 c_0^6} \int \frac{d^3 y}{|x-y|^2} \frac{I}{(1-M_c \cos \theta)^5} \frac{I}{2\pi} \\
&\times \int d\tau^* e^{i\omega\tau^*} Q(x, y, \tau) = \frac{I}{16\pi^2 c_0^6} \int \frac{d^3 y}{|x-y|^2} \frac{I}{(1-M_c \cos \theta)^5} \\
&\times \int d\tau^* e^{i\omega\tau^*} \int d\gamma Q(x, y, \gamma) e^{-i\gamma\tau} = \frac{I}{16\pi^2 c_0^6} \\
&\times \int \frac{d^3 y}{|x-y|^2} \frac{I}{(1-M_c \cos \theta)^4} Q^s[x, y, \omega(1-M_c \cos \theta)] \quad (10)
\end{aligned}$$

where

$$\begin{aligned}
Q^s[x, y, \omega(1-M_c \cos \theta)] &= \frac{(x_i - y_i)(x_j - y_j)(x_k - y_k)(x_l - y_l)}{|x-y|^4} \\
&\times \int d^3 \lambda \omega^4 (1-M_c \cos \theta)^4 P_{ijkl}^s[y, \lambda, \omega(1-M_c \cos \theta)]
\end{aligned}$$

Equation (10) demonstrates that the static autocorrelation function consists of dynamic effects of the form $(1-M_c \cos \theta)^{-4}$ associated with the motion of the turbulence and source effects associated with the integration of the source term Q^s in a frame of reference moving at the turbulence convection velocity. A similar interpretation exists for the flight and simulated forward flight solutions that will be derived in subsequent sections.

The one-third octave band SPL can now be defined from the power spectral density. Let ω_{ci} be the i th center frequency with upper and lower frequency limits ω_{ui} and ω_{li} , respectively. Then

$$\begin{aligned}
\text{SPL}_s(x, \omega_{ci}) &= 10 \log \int_{\omega_{li}}^{\omega_{ui}} \langle p_s^2(x, \omega) \rangle d\omega \\
&\equiv 10 \log [\langle p_s^2(x, \omega_{ci}) \rangle \Delta \omega_i]
\end{aligned}$$

where $\Delta \omega_i = \omega_{ui} - \omega_{li}$. Then using the equation for the power spectral density,

$$\begin{aligned}
\text{SPL}_s(x, \omega_{ci}) &= 10 \log \left[\frac{I}{16\pi^2 c_0^6} \int \frac{d^3 y}{|x-y|^2} \frac{I}{(1-M_c \cos \theta)^5} \right. \\
&\times \tilde{Q}^s(x, y, \omega_{ci}(1-M_c \cos \theta)) \left. \right] \quad (11)
\end{aligned}$$

where

$$\begin{aligned}
\tilde{Q}^s[x, y, \omega_{ci}(1-M_c \cos \theta)] \\
= \omega_{ci} (1-M_c \cos \theta) Q^s[x, y, \omega_{ci}(1-M_c \cos \theta)]
\end{aligned}$$

Equation (11) demonstrates that the sound measured at frequency ω_{ci} is related to the frequency $\omega_{ci}(1-M_c \cos \theta)$ in the turbulence-fixed frame of reference.

Subsonic Flight Jet Noise

Ffowcs Williams⁶ and Ribner⁷ have derived an expression analogous to Eq. (11) for an aircraft in subsonic flight with Mach number M_0 , referenced with respect to the ambient speed of sound. For a source moving from right to left, with M_0 parallel to M_c , as illustrated in Fig. 2, and referenced with respect to a nozzle-fixed coordinate frame, Eq. (1) is replaced by (see Ref. 8 for a definition of the appropriate Green's function)

$$\begin{aligned}
(\rho - \rho_0) \{x, t\} &= \frac{I}{4\pi c_0^2} \int \frac{d^3 y}{\sigma} \frac{\partial^2}{\partial x_i \partial x_j} T_{ij}^f(y, \tau_y) \\
\sigma &= |x - y_e| (1 + M_0 \cos \theta_e)
\end{aligned} \quad (12)$$

and

$$\tau_y = t - \frac{|x - y_e|}{c_0}$$

In Eq. (12) the subscript e denotes the retarded coordinate system, y_e is the position of the source turbulence at the time of sound emission, and the superscript f on T_{ij} is used to indicate that the source function in flight will differ from that in the static case. Figure 2 illustrates the emission coordinate system. The relationship between the angle of the aircraft when the sound is received θ and the emission angle θ_e is

$$\tan \theta = \sin \theta_e / (\cos \theta_e - M_0) \quad (13)$$

The transformations analogous to those in the preceding section [i.e., Eq. (8)] will be repeated. Using the transformation to the λ coordinate system, as in Eq. (8), and modifying Eq. (7) to $\Delta = \lambda + (M_c + M_0) \tau c_0$, where from Fig. 2, $M_c + M_0 = (M_c - M_0) x_l$, one obtains

$$\frac{\partial \tau_y}{\partial x_i} \equiv \frac{\partial \tau_z}{\partial x_i} = -\frac{I}{c_0} \frac{x_i - y_{ei}}{|x - y_e|} \frac{I}{1 + M_0 \cos \theta_e}$$

$$d^3 \Delta = d^3 \lambda (1 + M_0 \cos \theta_e) / [1 + (M_0 - M_c) \cos \theta_e]$$

and

$$\frac{\partial}{\partial \tau} R_{ijkl}^f(y, \Delta, \tau) = \frac{1 + M_0 \cos \theta_e}{1 + (M_0 - M_c) \cos \theta_e} \frac{\partial}{\partial \tau} P_{ijkl}^f(y, \lambda, \tau)$$

The autocorrelation function, calculated using Eq. (12) and following the same procedure outlined in the preceding section, is

$$\begin{aligned}
\langle p_f^2(x, t, \tau^*) \rangle &= \frac{I}{16\pi^2 c_0^6} \int \frac{d^3 y}{|x-y|^2} \frac{I}{1 + M_0 \cos \theta_e} \\
&\times \frac{I}{[1 + (M_0 - M_c) \cos \theta_e]^5} \\
&\times \frac{(x_i - y_{ei})(x_j - y_{ej})(x_k - y_{ek})(x_l - y_{el})}{|x-y|^4} \\
&\times \int d^3 \lambda \frac{\partial^4}{\partial \tau^4} P_{ijkl}^f(y, \lambda, \tau) \quad (14)
\end{aligned}$$

where the notation f denotes the flight solution, and $(x_i - y_{ei})/|x - y_e|$ are the measurement cosines referenced with respect to the acoustic emission angles. The t dependence has been included in $\langle p_f^2(x, t, \tau^*) \rangle$ because the source motion in a flyover test does not produce statistically stationary noise for the ground observer. The relationship between τ and τ^* is $\tau = \tau^* / [1 + (M_0 - M_c) \cos \theta_e] + 0(\lambda/c_0)$, which (as proved in the preceding section) implies a doppler shift in the frequency of the far-field noise with respect to the generating turbulence of $[1 + (M_0 - M_c) \cos \theta_e]^{-1}$.

If the flight data are ensemble averaged to remove the nonstationary character of the data, the procedure for calculating one-third octave band sound pressure level described in the preceding section can be used. Equation (14) implies that

$$\begin{aligned}
\text{SPL}_f(x, \omega_{ci}) &= 10 \log \left\{ \frac{I}{16\pi^2 c_0^6} \int \frac{d^3 y}{|x-y_e|^2} \right. \\
&\times \frac{\tilde{Q}^f(x, y_e, \omega_{ci} [1 + (M_0 - M_c) \cos \theta_e])}{(1 + M_0 \cos \theta_e) [1 + (M_0 - M_c) \cos \theta_e]^5} \left. \right\} \quad (15)
\end{aligned}$$

where $\tilde{Q}^f(x, y_e, \omega_{ci} [1 + (M_0 - M_c) \cos \theta_e])$ is given by Eq. (11) with suitable replacement of y by y_e , $(1 - M_c \cos \theta)$ by $[1 + (M_0 - M_c) \cos \theta_e]$, and the superscript s by the superscript f .

In the analysis to this point, the Lighthill source term has been used to develop the static and flight solutions. This source term was chosen because of its simplicity and because the focus of the current study is on the relationship of acoustic autocorrelations, one-third octave SPL, and (in Sec. III) overall sound pressure level (OASPL) in different static/flight environments. Other source terms could also be used, such as those of Michalke and Michel,⁴ who developed an acoustic formulation including temperature effects and assumptions regarding the stretching of a jet in an external flow. The source term Q_f in Eq. (15) is identical to the first term in Eq. (2.4) of their paper. The difference between the current study and Michalke and Michel's work is that their paper focused on the generalization of the source term, while the current study focuses on the dynamic transformation between the static and flight conditions.

Subsonic Forward Flight Simulation

In this section, the subsonic flight simulation solution analogous to Eqs. (11) and (15) is derived. The relevant geometry for a forward flight simulation is illustrated in Fig. 3. The jet exhaust nozzle is placed in a flow from left to right at a Mach number M_0 equal to the desired flight Mach number and parallel to the turbulence convection velocity M_c measured with respect to a nozzle-fixed coordinate system.

Figure 3 illustrates the relevant geometry for a simulated forward flight test in which the noise measurements are obtained in a wind tunnel mean flow. Often, however, the effect of the mean flow is simulated in a free-jet wind tunnel in which the noise measurements are separated from the noise generation region by a free-jet shear layer. As discussed in Ref. 9, a theoretical shear layer correction can be used to remove the refraction effect of the shear layer and the noise measurements then become equivalent to those obtained in a uniform mean flow.

From Refs. 10 and 11, the wave equation for aerodynamic sound generation in a medium with a uniform mean flow is, if the turbulence Mach number is small and the noise generated by turbulence is greater than the noise generated by entropy gradients in the turbulent flow,

$$\left(\nabla^2 - \frac{1}{c_0^2} \frac{D^2}{Dt^2}\right)\rho = \frac{\partial^2 T_{ij}^{sf}}{\partial x_i \partial x_j} \quad (16)$$

where

$$\frac{D}{Dt} = \frac{\partial}{\partial t} + M_0 c_0 \frac{\partial}{\partial x_i}$$

and the superscript sf on T_{ij} indicates that T_{ij} is to be evaluated in a simulated forward flight test.

The solution to Eq. (16) is then

$$(\rho - \rho_0)\{x, t\} = \frac{1}{4\pi c_0^2} \int \frac{d^3 y}{\sigma} \frac{\partial^2 T_{ij}^{sf}(y, \tau_y)}{\partial x_i \partial x_j} \quad (17)$$

where

$$\sigma = |x - y_e| (1 + M_0 \cos \theta_e)$$

and the relationship between the apparent source coordinate system $|x - y_e|$ and actual coordinate system $|x - y|$, illustrated in Fig. 3, is given by the same formula as in Eq. (13) and

$$\tau_y = t - \frac{|x - y_e|}{c_0}$$

Equation (17) can be used to calculate the mean square pressure in a simulated flight test using the same method developed in the preceding sections. In a simulated forward flight test, however, the relationship between the Δ and λ coordinate systems is given by $\Delta = \lambda + c_0 M_c \tau$. Then the transformations analogous to those in Eq. (8) are

$$\frac{\partial \tau_y}{\partial x_i} = \frac{\partial \tau_z}{\partial x_i} = -\frac{1}{c_0} \frac{x_i - y_{ei}}{|x - y_e|} \frac{1}{1 + M_0 \cos \theta_e}$$

$$d^3 \Delta = d^3 \lambda (1 + M_0 \cos \theta_e) / [1 + (M_0 - M_c) \cos \theta_e] \quad (18)$$

and

$$\frac{\partial}{\partial \tau} R_{ijkl}^{sf}(y, \Delta, \tau) = \frac{1 + M_0 \cos \theta_e}{1 + (M_0 - M_c) \cos \theta_e} \frac{\partial}{\partial \tau} P_{ijkl}(y, \lambda, \tau)$$

Then the autocorrelation function calculated using Eqs. (17) and (18) is given by

$$\begin{aligned} \langle p_{sf}^2(x, \tau^*) \rangle &= \frac{1}{16\pi^2 c_0^2} \int \frac{d^3 y}{|x - y_e|^2} \\ &+ \frac{(x_i - y_{ei})(x_j - y_{ej})(x_k - y_{ek})(x_l - y_{el})}{|x - y_e|^4 (1 + M_0 \cos \theta_e)} \\ &\times \frac{1}{[1 + (M_0 - M_c) \cos \theta_e]^5} \int d^3 \lambda \frac{\partial^4}{\partial \tau^4} P_{ijkl}^{sf}(y, \lambda, \tau) \end{aligned} \quad (19)$$

where the notation sf was used to denote the simulated forward flight solution. The relationship between τ and τ^* is $\tau = \tau^* (1 + M_0 \cos \theta_e) / [1 + (M_0 - M_c) \cos \theta_e] + 0(\lambda/c_0)$, which implies a doppler shift of $(1 + M_0 \cos \theta_e) / [1 + (M_0 - M_c) \cos \theta_e]$ from the turbulence-fixed frame to the observer-fixed frame.

Using the procedure defined in the section summarizing the analysis of static jet noise, the one-third octave band SPL can be calculated using Eq. (19). The result is

$$\begin{aligned} \text{SPL}_{sf}(x, \omega_{ci}) &= 10 \log \left\{ \frac{1}{16\pi^2 c_0^2} \int \frac{d^3 y}{|x - y_e|^2} \frac{1}{1 + M_0 \cos \theta_e} \right. \\ &\times \frac{1}{[1 + (M_0 - M_c) \cos \theta_e]^5} \\ &\times \tilde{Q}^{sf} \left[x, y_e, \omega_{ci} \frac{1 + (M_0 - M_c) \cos \theta_e}{1 + M_0 \cos \theta_e} \right] \left. \right\} \end{aligned} \quad (20)$$

where \tilde{Q}^{sf} is given by Eq. (11) with suitable replacement of y by y_e , $(1 - M_c \cos \theta) \omega_{ci}$ by $[1 + (M_0 - M_c) \cos \theta_e] \omega_{ci} / (1 + M_0 \cos \theta_e)$, and the superscript s by the superscript sf .

III. Comparison of Solutions

The three possible transformations of jet noise data are presented below based on a comparison of Eqs. (11), (15), and (20).

1) Static to flight. The procedure for a prediction of the flyover one-third octave band sound pressure level from static measurements can be obtained from Eqs. (11) and (15). If static measurements at θ_e are compared with flight measurements at θ , where the relationship between θ and θ_e is given by Eq. (13), then in the far field,

$$\begin{aligned} \text{SPL}_f(x, \theta, \omega_{ci}) &= \text{SPL}_s \left(x, \theta_e, \omega_{ci} \frac{1 + (M_0 - M_c) \cos \theta_e}{1 - M_c \cos \theta_e} \right) \\ &+ 10 \log \left(\frac{1 - M_c \cos \theta_e}{1 + (M_0 - M_c) \cos \theta_e} \right)^5 \frac{1}{1 + M_0 \cos \theta_e} \\ &+ \frac{\{d^3 y \tilde{Q}^f\{x, y_e, \omega_{ci} [1 + (M_0 - M_c) \cos \theta_e]\}\}}{\{d^3 y \tilde{Q}^s\{x, y_e, \omega_{ci} [1 + (M_0 - M_c) \cos \theta_e]\}\}} \end{aligned} \quad (21)$$

In deriving this result it is assumed that, in spite of the source motion with respect to the observer in a flight test, the measured noise will be statistically stationary. This assumption can be realized experimentally by ensemble-averaging noise measurements from multiple microphones in a flyover test.

2) Static to simulated forward flight. The procedure for prediction of simulated forward flight measurements from static measurements can be obtained from Eqs. (11) and (20). If static measurements at θ_e are compared with simulated forward flight measurements at θ , then

$$\begin{aligned} \text{SPL}_{sf}(x, \theta, \omega_{ci}) = & \text{SPL}_s \left(x, \theta_e, \omega_{ci} \frac{1 + (M_0 - M_c) \cos \theta_e}{(1 + M_0 \cos \theta_e)(1 - M_c \cos \theta_e)} \right) \\ & + 10 \log \left\{ \left(\frac{1 - M_c \cos \theta_e}{1 + (M_0 - M_c) \cos \theta_e} \right)^5 \frac{1}{1 + M_0 \cos \theta_e} \right. \\ & \times \left. \frac{\int d^3 y \tilde{Q}^{sf}(x, y_e, \omega_{ci} \frac{1 + (M_0 - M_c) \cos \theta_e}{1 + M_0 \cos \theta_e})}{\int d^3 y \tilde{Q}^s(x, y_e, \omega_{ci} \frac{1 + (M_0 - M_c) \cos \theta_e}{1 + M_0 \cos \theta_e})} \right\} \quad (22) \end{aligned}$$

3) Simulated forward flight to flight. The procedure for prediction of flight measurements from simulated forward flight measurements can be defined from Eqs. (15) and (20). If flight and simulated forward flight measurements are compared at the same angle, then

$$\begin{aligned} \text{SPL}_f(x, \theta, \omega_{ci}) = & \text{SPL}_{sf}(x, \theta, \omega_{ci} (1 + M_0 \cos \theta_e)) \\ & + 10 \log \left\{ \frac{\int d^3 y \tilde{Q}^f(x, y_e, \omega_{ci} [1 + (M_0 - M_c) \cos \theta_e])}{\int d^3 y \tilde{Q}^{sf}(x, y_e, \omega_{ci} [1 + (M_0 - M_c) \cos \theta_e])} \right\} \quad (23) \end{aligned}$$

If the volume integrals in Eqs. (21-23) are known, then the transformations between the three types of measurements are well defined. Measurement of the turbulence properties of a jet allow the integrals to be evaluated. A crude example of this is found in Ref. 12, in which the ratio in Eq. (22) was measured experimentally and found to be approximated by

$$\frac{\int d^3 y \tilde{Q}^{sf}(x, y_e, \omega_{ci} \frac{1 + (M_0 - M_c) \cos \theta_e}{1 + M_0 \cos \theta_e})}{\int d^3 y \tilde{Q}^s(x, y_e, \omega_{ci} \frac{1 + (M_0 - M_c) \cos \theta_e}{1 + M_0 \cos \theta_e})} \cong (1 - m)^{5.8} \sqrt{1 + m}$$

where m is the ratio of the flight to turbulence convection velocity.

In many studies it has been assumed that the flight and simulated flight volume integrals are identical, in which case the relationship between the flight and simulated forward flight SPL measurements is very simple, requiring only a doppler shift in frequency of the form $(1 + M_0 \cos \theta_e)^{-1}$. The assumption that the integrals are the same is approximately true because of the expected similarity of the turbulence parameters in the two cases. However, in most wind tunnel forward flight simulations, the initial boundary-layer thickness at the nozzle exit plane will be substantially different than the initial boundary thickness in a flight test, and the assumption is not entirely correct (see Ref. 13).

Equations (22) and (23) can be used to analyze the role of relative velocity exponents (see Ref. 9, for example) in flyover noise predictions. Exponents n are calculated from static and simulated forward flight jet noise data. They are defined by the formula

$$n = \frac{\text{OASPL}_{sf}(x, \theta) - \text{OASPL}_s(x, \theta_e) + 10 \log(1 + M_0 \cos \theta_e)}{10 \log(V_j - V_0) / V_j} \quad (24)$$

where V_j is the jet exhaust velocity, OASPL is the overall sound pressure level, which is obtained from the one-third octave band sound pressure level by antilogarithmically summing the SPL levels from 50 to 10,000 Hz, and the subscripts s and sf indicate the static and simulated forward flight measurements, respectively. If it is assumed that the

change in the jet noise level is independent of frequency, then

$$\begin{aligned} \text{OASPL}_{sf}(x, \theta) - \text{OASPL}_s(x, \theta_e) & \cong \text{SPL}_{sf}(x, \theta, \omega_{ci}) \\ & - \text{SPL}_s(x, \theta_e, \omega_{ci}) \end{aligned}$$

From this result, Eq. (24) implies that

$$10 \log \left[\left(\frac{1 - M_c \cos \theta_e}{1 + (M_0 - M_c) \cos \theta_e} \right)^5 \frac{\int d^3 y \tilde{Q}^{sf}}{\int d^3 y \tilde{Q}^s} \right] = 10 \log \left(\frac{V_j - V_0}{V_j} \right)^n$$

Then with the additional assumption that $\int d^3 y \tilde{Q}^{sf} = \int d^3 y \tilde{Q}^f$, Eq. (21) can be written

$$\begin{aligned} \text{SPL}_f(x, \theta, \omega_{ci}) = & \text{SPL}_s \left(x, \theta_e, \omega_{ci} \frac{1 + (M_0 - M_c) \cos \theta_e}{1 + M_0 \cos \theta_e} \right) \\ & + 10 \log \left(\frac{V_j - V_0}{V_j} \right)^n \end{aligned}$$

This expression is the basis of most flight jet noise prediction systems, but, as the preceding analysis indicates, it involves many assumptions.

IV. Conclusions

The relationships between static, flight, and simulated forward flight measurements were defined using Lighthill's acoustic analogy. The effects of measuring noise in different reference frames can be divided into two areas: dynamic effects associated with the source and medium motion, which are defined by the Green's functions for the solutions in different coordinate frames, and source effects arising from the effect of motion on the noise source. Transformation of the noise measurements from the static to the flight coordinate frame requires the inclusion of both effects whereas, under the appropriate conditions, transformation of noise measurements from the simulated forward flight to the flight coordinate frame requires only a doppler shift in frequency.

References

- Cocking, B. J. and Bryce, W. D., "Subsonic Jet Noise in Flight Based on Some Recent Wind Tunnel Results," AIAA Paper 75-462, 1975.
- Morfe, C. L. and Tester, B. J., "Noise Measurements in a Free Jet, Flight Simulation Facility: Shear Layer Refraction and Facility to Flight Corrections," AIAA Paper 76-531, 1976.
- Crighton, D. G., Ffowcs Williams, J. E., and Cheeseman, I. C., "The Outlook for Simulation of Forward Flight Effects on Aircraft Noise," AIAA Paper 76-530, 1976.
- Michalke, A. and Michel, U., "Predictions of Jet Noise in Flight from Static Tests," *Journal of Sound and Vibration*, Vol. 67, 1979, pp. 341-367.
- Lighthill, M. J., "On Sound Generated Aerodynamically, I: General Theory," *Proceedings of the Royal Society of London*, Vol. 211A, 1952, pp. 564-587.
- Ffowcs Williams, J. E., "The Noise from Turbulence Convected at High Speed," *Proceedings of the Royal Society of London*, Vol. 255A, 1963, pp. 469-503.
- Ribner, H. S., "Aerodynamic Sound from Fluid Dilation," Institute of Aerospace Studies, University of Toronto, Canada, Rept. 86, 1962.
- Morse, P. M. and Ingard, K. U., *Theoretical Acoustics*, McGraw Hill Book Co., New York, 1968.
- Packman, A. B., Ng, K. W., and Paterson, R. W., "Effect of Simulated Forward Flight on Subsonic Jet Noise Measurements," *Journal of Aircraft*, Vol. 13, 1976, pp. 1007-1013.
- Howe, M. S., "Contributions to the Theory of Aerodynamic Sound, with Application to Excess Jet Noise and the Theory of the Flute," *Journal of Fluid Mechanics*, Vol. 71, Pt. 4, 1975, pp. 625-673.
- Howe, M. S., "Attenuation of Sound in a Low Mach Number Nozzle Flow," *Journal of Fluid Mechanics*, Vol. 91, Pt. 2, 1979, pp. 209-229.
- Larson, R. S., McColgan, C. J., and Packman, A. B., "Jet Noise Source Modification Due to Forward Flight," *AIAA Journal*, Vol. 16, March 1978, pp. 225-232.
- Sarohia, V. and Massier, P. F., "Effects of External Boundary Layer Flow on Jet Noise in Flight," AIAA Paper 76-558, 1976.